BEU Journal of Science
8 (4), 1194-1202, 2019

Araştırma Makalesi / Research Article

Investigation of Thermodynamic Properties of $Ni_{30}Ti_{50}Cu_{20}$ Shape Memory Alloy

Ercan ERCAN[1*], Fethi DAĞDELEN[2], Mediha KÖK[2], Esra BALCI[2]

[1]*Bitlis Eren University, Faculty of Science, Department of Physics, Bitlis*
[2]*Firat University, Faculty of Science, Department of Physics, Elazığ*
(ORCID: 0000-0002-1583-6068) (ORCID: 0000-0001-9849-590X)
(ORCID: 0000-0001-7404-4311) (ORCID: 0000-0003-0127-7602)

Abstract
In this study, after producing $Ni_{30}Ti_{50}Cu_{20}$ shape memory alloy by using arc melting technique, some examination was performed, including phase transformation temperatures, microstructural features, and certain thermodynamic parameters. The DSC thermogram run with 10°C/min heating-cooling rate, and thus it was determined that austenite start (A_s) temperature is 23.5 °C, austenite finish (A_f) temperature is 50.6 °C, martensite start (M_s) temperature is 26.7 °C and martensite finish (M_f) temperature is -0.10 °C. For different heating rate of DSC measurements, it was observed that martensite to austenite phase transformation temperatures (A_s and A_f) are changed, while it did not effect on the reversible martensite phase transformation temperature (M_s and M_f). Thermal activation energy of the alloy was measured by Kissinger method, which is E_a=63.208 kJ/mol. Moreover, Gibbs free energy was slightly increased with increasing heating-cooling rates. The DSC curves and XRD crystal analysis showed the phase transformation was occurred in a single step B2 ↔B19. Beside, some precipitations like Ti_2(Ni, Cu) as well as matrices in the form of $TiNi_{0.8}Cu_{0.2}$ of element Cu dissolved in interphases of NiTi were encountered. SEM-EDX was used to determine chemical composition of Ti_2(Ni, Cu) phase in atomic percentage (at.%). The microhardness of the alloy was 219 HV, where Cu element was added to makes alloy to be softer than the traditional binary NiTi alloys.

Keywords: shape memory alloy, transformation temperature, microstructure.

Şekil Hatırlamalı $Ni_{30}Ti_{50}Cu_{20}$ Alaşımının Termodinamik Özelliklerinin İncelenmesi

Öz
Şekil hatırlamalı NiTiCu alaşımı ark-ergitme yöntemi ile üretildi ve faz dönüşüm sıcaklıkları, bazı termodinamik parametreleri ile mikroyapısal özellikleri araştırıldı. 10°C/dak. ısıtma-soğutma hızı ile alınan DSC sonuçlarına göre; austenite başlangıç sıcaklığı (A_s) 23.5 °C, austenite bitiş sıcaklığı (A_f) 50.6 °C, martensit başlangıç sıcaklığı (M_s) 26.7 °C ve (M_f) -0.10 °C olarak bulundu. Farklı ısıtma hızlarında alınan DSC ölçümlerine göre ise alaşımın martensit fazdan austenite faza geçerken dönüşüm sıcaklıkları (A_s ve A_f) değişirken, austenite fazdan martensit faza geçerken dönüşüm sıcaklıklarının (M_s ve M_f) değişmediği görülmüştür. Kissinger metodu ile bulunan aktivasyon enerjisi E_a=63.208 kJ/mol olarak bulunmuştur. Gibbs serbest enerjisi ısıtma-soğutma hızlarıyla küçük değişimler göstermiştir. DSC eğrilerinden tek-adımlı B2 ↔B19 faz geçişi görülmüş ve bu fazların kristal yapıları XRD analizi ile belirlenmiştir. Bununla birlikte Ti_2(Ni, Cu) çökeltilerinin yanı sıra NiTi alaşımının interfazlarında çözünen Cu elementlerinin $TiNi_{0,8}Cu_{0,2}$ formundaki matrislerine rastlanmıştır. SEM-EDX sonuçları ile alaşımdaki Ti_2(Ni, Cu) çökeltilerinin atomik yüzdeleri belirlenmiştir. Alaşımın mikrosertliği 219 HV olarak bulunmuştur. Bu değer, artan Cu miktarının geleneksel ikili NiTi alaşımlarını daha yumuşak materyal haline getirdiğini göstermiştir.

Anahtar kelimeler: Şekil hatırlamalı alaşım, dönüşüm sıcaklıkları, mikroyapı.

[*]Sorumlu yazar: eercan@beu.edu.tr
Geliş Tarihi: 25.03.2019, Kabul Tarihi: 08.07.2019

1. Introduction

NiTi-based shape memory alloys (SMAs) are well known for unique shape memory effect (SME), super-elasticity, and damping capacity. In addition, thanks to high ductility features, these alloys are started to be used frequently in engineering applications such as transportation vehicles, building constructions and pipe couplings to facilitate vibration dampening [1-3]. However, due to some drawbacks of these alloys, they are not suitable for being used in actuator field [4, 5]. To eliminate the problems, thermo-mechanical properties of NiTi-based shape memory alloys (SMAs) are aimed to be improved. Some of these studies include modifying transformation temperatures, yield strength, fatigue life and transformation hysteresis width. Studies to improve transformation temperatures and hysteresis width are still continued frequently. Binary NiTi alloys are carried out with ternary and quaternary elements to reach the desired properties [6]. It is known that especially copper element added instead of Ni element reduces transformation temperature hysteresis and increases strength differences between parent and martensite phases. In addition to this, it is known that adding Cu element to binary NiTi alloy increases the number of cycles, and displays more stable transformation temperature after mechanical deformation, removes R phase, boosts fatigue resistance with thermal cycles, and lowers super-elastic hysteresis strain. As a result of these improvements, NiTiCu SMAs become useful in many applications such as actuators [5, 7]. Furthermore, it is known that replacing Cu element instead of Ni element in NiTi alloy, M_s transformation temperature lowers the composition sensitivity, pseudo elasticity of hysteresis, flow stress level in martensite state and prevents the precipitations of X-phase of (Ti_3Ni_4) [8, 9]. With the reduction of precipitations, it is known that the number of cycles within the alloy is raised. Therefore, $Ti_{50}Ni_{50-x}Cu_x$ ($7.5 \leq x \leq 25$) alloys are substantially interesting. In contrast to increasing value of x in $Ti_{50}Ni_{50-x}Cu_x$ alloy, temperature hysteresis will be decreased, which makes it to be used as actuator better than NiTi alloy. The phase transformation straightly depends on the rate of third constituent composition element, where by adding $x < 5$, $5 \leq x \leq 20$ and $x > 20$ at%, it is found that they display phase transformations as B2↔B19′, B2↔B19↔B19′ and B2↔B19, respectively. Here B2 (cubic) is the main phase, B19 and B19′ are orthorhombic and monoclinic martensite phases [1, 4, 5, 10-12]. Although B19 martensite phase is formed in alloys cast in the amount of 5 at % Cu, B19′ martensite phase occurs in alloys cast in the amount of 7.5 with 15 at. % Cu. The given amount of 10 and 20 at.% Cu causes to phase transform from B2 to B19, and thus the elastic modulus is decreased [6]. It is known that B19 martensite phase is formed again in alloys with the amount of 20 at.% Cu [12]. Recently, some new researches have been conducted on NiTiCu-based alloys by adding fourth different elements such as Hf, Pd, Y, Zr, and Nb [13-18]. In this respect, NiTiCu alloys were reexamined to eliminate their thermal deficiencies (such as thermal activation energy) and compare the results with literature.

In this study, NiTiCu (30:50:20 at. %) alloy was produced. As well as thermodynamic parameters such as transformation temperatures, transformation hysteresis range, thermal activation energy, phase transformation enthalpy, entropy changes, microstructures, and mechanic properties of produced alloy were examined.

2. Materials and Methods

Metal powders (30at. % Ni, 50at. % Ti, 20at. % Cu) with 99.9% purity were mixed. Then, the metal powders were pressed to make pellets with a diameter of 13 mm. They were produced by arc-melting system under argon atmosphere to obtain NiTiCu alloy. The ingot remelted for five times to be more homogenize. A 50 mg specimen was utilized for DSC (Differential Scanning Calorimetry) measurement to find phase transformation temperatures and some related thermodynamic parameters, such as latent heat of phase transformation (enthalpy change). DSC measurements was carried out for both A→M and M→A process at rate of 10, 15, 20 and 25 °C/min. The microstructures was investigated with optical microscopy (OM). For surface morphology observation, the sample was polished and chemically etched in a solution of ($HF+NOH_3+H_2O$-1:2:5) for 10 sec. for The crystal structure analysis, XRD measurement ($Cu_{K\alpha}$=1.543nm) was performed at a scanning rate of 4°/min. from 30° to 80° at room temperature. Vickers hardness test was performed to measure the hardness of the alloy. Microstructural and elemental analysis measurements were made at room temperature by SEM-EDX (Scanning Electron Microscopy with Energy Dispersive X-ray Spectroscopy) measurement.

3. Results and Discussion

3.1. Differential Scanning Calorimetry

Thermal properties of $Ni_{30}Ti_{50}Cu_{20}$ SMA, which produced by arc-melting method, were investigated by DSC measurement method. For DSC measurements, heating-cooling rate were chosen as 10 ºC/min, 15 ºC/min, 20 ºC/min and 25 ºC/min, where the acquired phase transformation curves and transformation temperature values were given in Figure 1 and Table 1. According to DSC results, it is clear that $Ni_{30}Ti_{50}Cu_{20}$ SMA displays a B2↔B19 of phase transformation at one-step, without an intermediate phase such as R-Phase. Heating-cooling scanning at 10 ºC/min perceived more heating and cooling and took a prolific measurement and, thus the ideal heating rate was found as 10 ºC/min [2, 6]. Therefore, the DSC measurement with heating/cooling rate of 10 ºC, has been chosen as reference to compare the obtained phase transformation temperatures with literature and according to the obtained results, transformation temperatures of the alloy were determined as A_s = 23.5, A_f = 50.6, M_s= 26.7, M_f = -0.10 ºC. The obtained transformation temperatures have a small change with the values found in literature [19]. In literature, it has been seen that M_s temperature changes from 40 °C to -20 °C for NiTiCu alloy that include Cu amount between 5-15 (at%), while for addition of 15-20 (at%) of Cu, M_s varies from 40 to -60°C [12]. The reasons of differences between our study and literature can be explained such that: Microstructure of the alloy depends on the production technique, rate of purity of elements, and a resistance surface potential that put up against transformation [8, 20, 21]. In addition, since dendrite structures can be seen in the SEM and optical microscope images, so it can be notice that the alloy was not completely homogenized during production process even after five times re-melted by arc melting furnace. Type of phase transformation process is another crucial parameter that straightly depends on the amount of Cu, e.g. Cu≤7,5:B2→B19', 7,5<Cu≤15: B2→B19→B19', Cu≥15: B2→B19 [12]. In addition, Figure 1 and Figure 2 clearly indicate that with increasing heating-cooling rate, the martensite phase temperatures (M_s and M_f) are constant, while austenite phase temperatures (A_s and A_f) dramatically increased. Also, is it found that austenite phase from B2 phase is transformed to B19 phase. The same result has been reported by Wang et al. for different heating/cooling rats [22]. On the other hand, with increasing heating rate, it was seen that transformation hysteresis (H_t=A_p-M_p) was increased. Phase transformation enthalpies depend on different heating-cooling rates, while the Gibbs free energies are almost the same. Also, when phase transformation temperatures are generally evaluated, NiTi alloy added Cu can be said to include both austenite and martensite structure at room temperature (~25 ºC). Accordingly, the values of enthalpy change for B2↔B19 are listed in Table 2. Gibbs free energy (driving force) required for initiating of nucleation of martensite phase are calculated by using the following formula:

$$\Delta G_{M\rightarrow A} = \Delta H_{M\rightarrow A} \Delta T / T_0 \qquad (1)$$

here ΔT = T_o-M_s, and T_o represents the temperature where Gibbs energy is equal to zero and it can be calculated with T_o = (A_f + M_s)/2 [23, 24]. For heating rates of 10, 15, 20, 25 °C/min, the Gibbs free energy was obtained as -1.24, -1.34, -1.45 and -1.56 Joule, respectively. When examined driving force values required for different heating rates, even though values are close to each other, it is seen that as the heating rate is increased, this value seems to display a slightly increase. This result is backed up with overlapping of transformation curves from austenite to martensite phase (during cooling process) in DSC curves. It is due to the fact that an internal stress has been induced during phase transformation from austenite to martensite in Gibbs free energy occurs at the same rate [25].

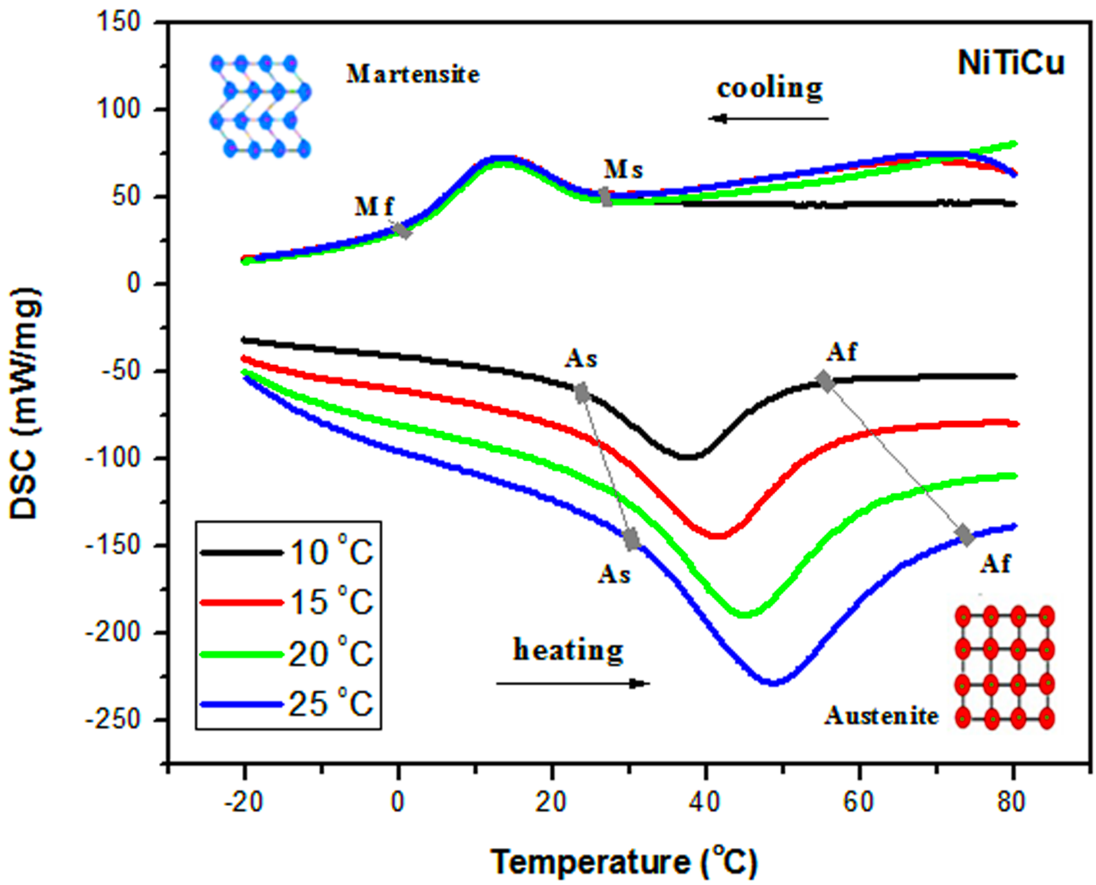

Figure 1. DSC curves of $Ni_{30}Ti_{50}Cu_{20}$ alloy obtained with different heating-cooling rate.

Table 1. Transformation temperatures as a function of heating-cooling rate for NiTi-20Cu SMA.

Heating-cooling rate	A_s (ºC)	A_f (ºC)	A_p (ºC)	M_s (ºC)	M_f (ºC)	M_p (ºC)	H_t (ºC)
10 ºC/min	23.5	50.6	37.9	26.7	-0.1	13.6	24.3
15 ºC/min	26.6	57.6	41.7	26.6	0.0	13.6	28.1
20 ºC/min	27.1	64.7	45.4	25.9	0.1	13.6	31.8
25 ºC/min	30.6	65.8	48.7	26.4	0.0	13.6	35.1

In addition, entropy values of martensite to austenite phase transformation is another thermodynamic parameter, which was calculated by the following expression [26-28];

$$\Delta S_{M\rightarrow A} = \Delta H_{M\rightarrow A}/T_0 \tag{2}$$

and

$$\Delta S_{A\rightarrow M} = \Delta H_{A\rightarrow M}/T_0 \tag{3}$$

here ΔS is entropy; $\Delta H_{M\rightarrow A}$ and $\Delta H_{A\rightarrow M}$ are the energy required for austenite and martensite phase transformation, respectively. The calculated values were listed in Table 2. Accordingly, A_f is increased with increasing speed of heating-cooling rate, thus its value directly influences on entropy change values. The impact of heating/cooling rate on phase transformation temperatures are demonstrated in Figure 3. There are different methods for calculating thermal activation energy, which needs for phase transformation. To calculate thermal activation energy (E_a) of B19→B2, maximum points of austenite phase peak T_m (A_p) obtained at heating rate of 10, 15, 20 and 25 °C were specified and listed in Table 2, and then Kissinger Method was used to obtain E_a [29, 30]:

$$\mathrm{d}\ln(\beta/Tm^2)/d(1/T) = -Ea/R \tag{4}$$

here, R is universal gas constant and β is heating rate. Graph of ln(β /T_m^2)-1000/T were drawn by utilizing Eq. 4 (Figure 3). Thermal activation energy of NiTiCu alloy was found as 63.208 kJ/mol. A greater values have been reported for activation energy of NiTi SMA compared to $Ni_{30}Ti_{50}Cu_{20}$ SMA added Cu [31, 32], which means $Ni_{30}Ti_{50}Cu_{20}$ SMAs needs lower activation energy than binary NiTi SMAs found in literature. The low activation energy indicates that the alloy need low energy for phase transformation from austenite to martensite and vice versa.

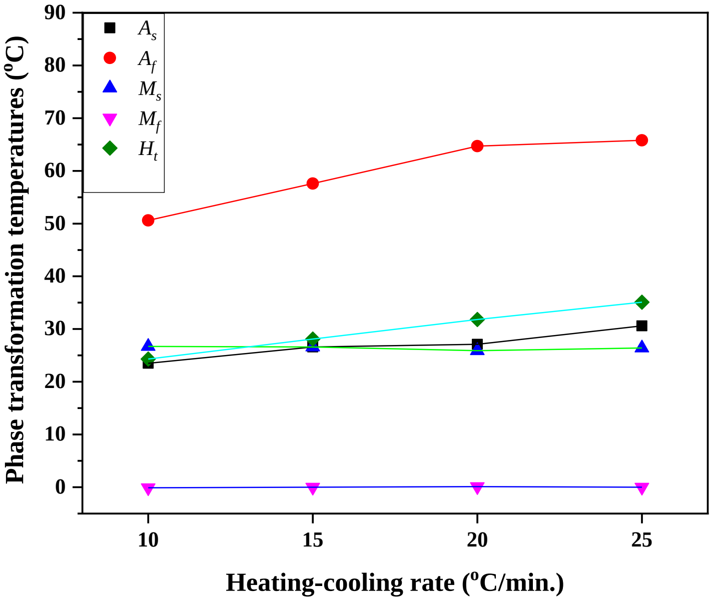

Figure 2. Change of transformation temperatures and transformation hysteresis of $Ni_{30}Ti_{50}Cu_{20}$ SMA for different heating-cooling rate

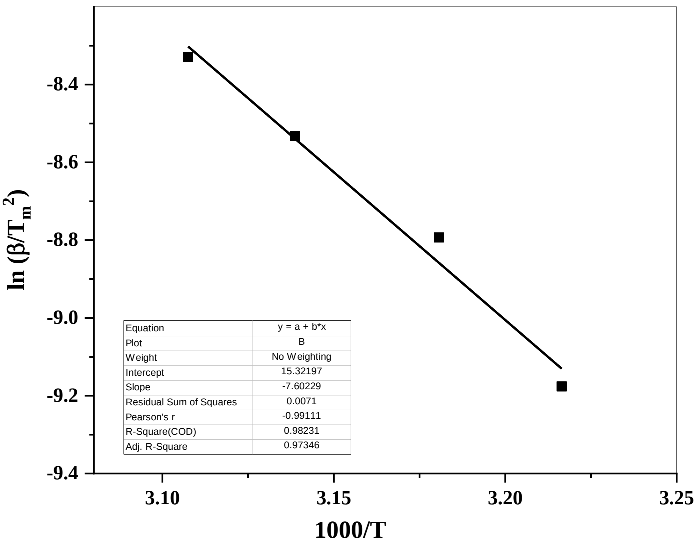

Figure 3. The ln(β/T_m^2)-1000/T plot drawn to calculate of thermal activation energy.

Table 2. Some thermodynamic parameters determined by different heating-cooling rates of NiTi-20Cu SMA.

	heating-cooling rate			
Thermodynamic parameters	**10 °C**	**15 °C**	**20 °C**	**25 °C**
A_p (K)	310,9	314,4	318,6	321,8
T_0 (°C)	38,65	42,1	45,3	46,1
$\Delta H_{A\rightarrow M}$ (J g^{-1})	5,22	4,80	6,13	4,80
$\Delta H_{M\rightarrow A}$ (J g^{-1})	-4,04	-3,64	-3,40	-3,66
$\Delta S_{M\rightarrow A}$ (mJ g^{-1} °C^{-1})	-0,104	-0,086	-0,075	-0,079
$\Delta S_{A\rightarrow M}$ (mJ g^{-1} °C^{-1})	0,135	0,114	0,135	0,104

3.2. Microstructure and Hardness

SEM image of NiTiCu alloy is demonstrated in Figure 4a. From the image some beadlike alignments within the structure can be seen. Likewise, these microstructures can be seen in optical microscope images (Figure 4b). Although grains and martensite plates are not observed within the structure (since this alloy is not completely in the form of martensite phase at room temperature), a large number of dendritic structures are monitored. Dendrites are aligned with the shape of bead and arranged in long-distance. Some dendrites are parallel within the matrix structure and overlap each other in some regions. EDX results obtained for some region on the surface of the alloy, which determined on SEM image (Figure 4a). It is known that precipitations occurring in alloy are Ti_2Ni phase. This precipitated phase was determined by the atomic ratio found by EDX. As opposed to the rate of element Ti, the rate of elements Ni and Cu is approximately 2:1. Therefore, content of Cu and Ni within the main phase of B2 is less available than Ti content. Adding Cu element to NiTi alloy modify the martensite structure, and is a factor to form orthorhombic B19 phase. Phase of Ti_2(Ni, Cu) within the structure have been determined in SEM-EDX analysis. One of the main parameters in terms of determining mechanic properties in the alloys is microhardness measurement. $Ni_{30}Ti_{50}Cu_{20}$ alloy recorded microhardness with 219 HV value. It can be concluded that adding Cu into NiTi alloy made it softer compared to the result obtained in literature [33]. Thus the formability of NiTiCu alloy is enhanced, due to the change in microstructure morphology within the alloy by adding element Cu [33].

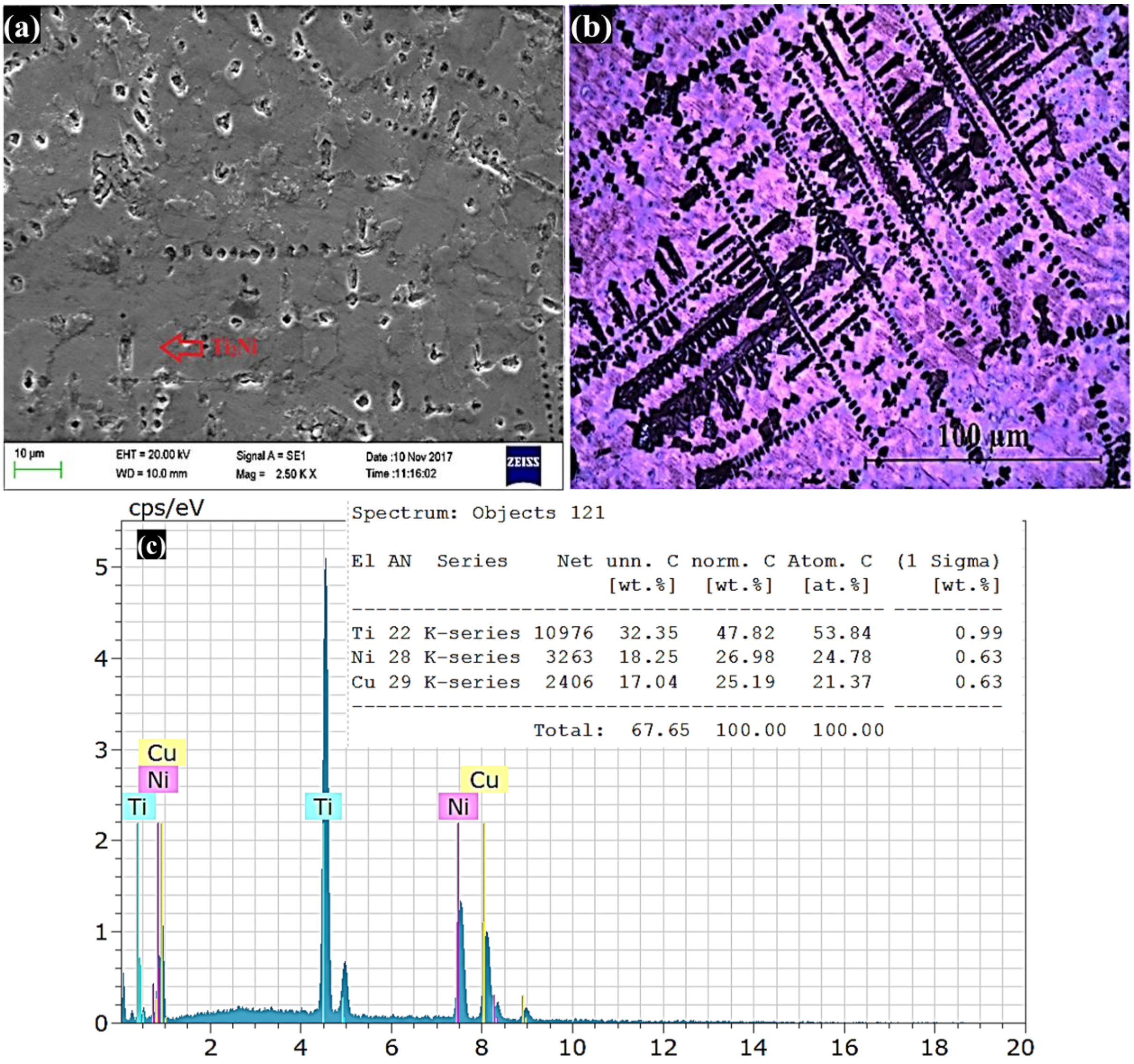

Figure 4. a) Optic micrograph, b) SEM image, and c) EDX results of NiTi-20Cu SMA

3.3. X-ray Diffraction

The analysis of X-ray diffraction for NiTiCu SMA can be seen in Figure 5. The pattern was obtained at room temperature, which enabled austenite and martensite phases to be observed together. In addition to the both B2 (cubic) and B19 (orthorhombic) phases, another precipitation is $Ti_2(Ni, Cu)$ that has a very sharp diffraction peaks. It is known that this precipitation influences transformation phase. The existence of B2, B19 and Ti_2Ni precipitation is supported by EDX result too. On the other hand, Ti_3Ni_4 precipitation phase is one of the reason for formation of R-phase, and since, its amount is too low, so R-phase in the DSC curves was not detected. Furthermore, Cu element dissolved within the interphase of NiTi and can be found in $TiNi_{0,8}Cu_{0,2}$ matrix [3, 4, 10, 34].

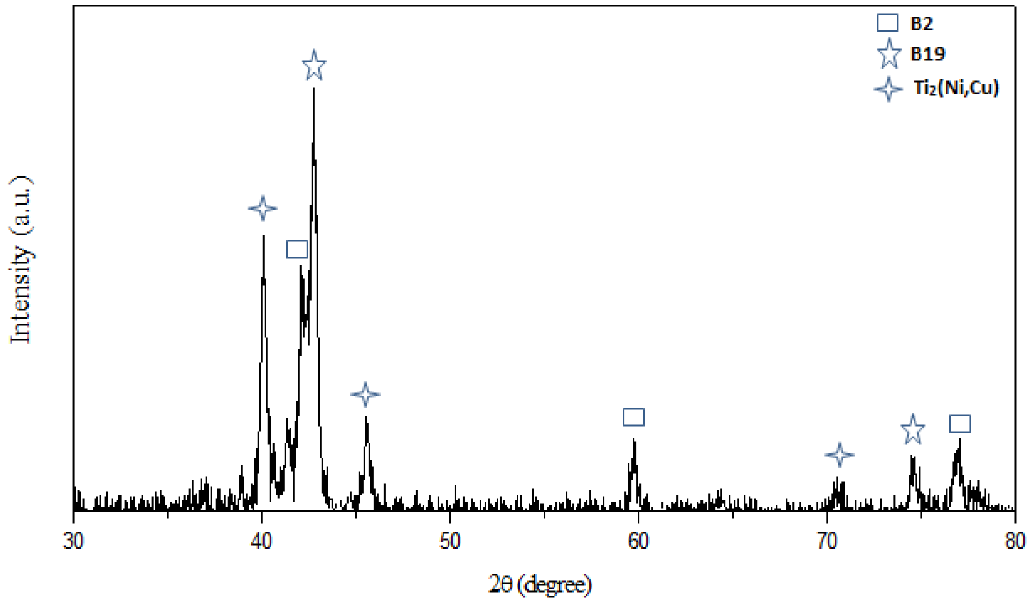

Figure 5. XRD pattern of NiTi-20Cu SMA.

4. Conclusions

The findings of this study suggest that NiTiCu (30:50:20 at. %) SMA alloy has displayed one-step phase transformation (B2↔B19) and by increasing heating rate, the transformation temperatures from austenite to martensite phase have not changed. Besides, with the increase of heating-cooling rate, hysteresis range has increased and thus it can be said that the alloy can be used widely as actuator. The evidence from this study point out the idea that adding 20 at. % Cu element has decreased the formation of Ti_3Ni_4 precipitation phase in the NiTi alloys, and thus R-phase was disappeared completely. This paper demonstrated that $Ni_{30}Ti_{50}Cu_{20}$ alloy has a lower activation energy compared to the conventional binary NiTi alloys. From the results it is found that surplus of Cu ratio may facilitate the process ability of the alloy.

Acknowledgements

This work was supported by Management Unit of Scientific Research projects of Firat University (FUBAP) (Project Number: FF. 16.41).

References

[1] Lin K.N., Wu S.K., Tsai C.L. 2008. The Effect of Thermal Cycling on B2→B19→B19' Transformations of $Ti_{50}Ni_{40}Cu_{10}$ Shape Memory Alloy by Dynamic Mechanical Analyzer. Materials Transactions, 49 (12): 2776-2780.

[2] Gil F.J., Solano E., Pena J., Engel E., Mendoza A., Planell J.A. 2004. Microstructural, mechanical and citotoxicity evaluation of different NiTi and NiTiCu shape memory alloys. Journal of Materials Science: Materials in Medicine, 15 (11): 1181-1185.

[3] Fan G., Zhou Y., Otsuka K., Ren X., Nakamura K., Ohba T., Suziki T., Yoshida I., Yin F. 2006. Effects of frequency, composition, hydrogen and twin boundary density on the internal friction of $Ti_{50}Ni_{50-x}Cu_x$ shape memory alloys. Acta Materialia, 54 (19): 5221-5229.

[4] Ohba T., Taniwaki T., Miyamoto H., Otsuka K., Kato K. 2006. In situ observations of martensitic transformations in $Ti_{50}Ni_{34}Cu_{16}$ alloy by synchrotron radiation. Materials Science and Engineering: A, 438-440: 480-484.

[5] Morakabati M., Aboutalebi M., Kheirandish Sh., Karimi T.A., Abbasi S.M. 2011. Hot tensile properties and microstructural evolution of as cast NiTi and NiTiCu shape memory alloys. Materials & Design, 32 (1): 406-413.

[6] Tang W., Sandström R., Wei Z.G., Miyazaki S. 2000. Experimental investigation and thermodynamic calculation of the Ti-Ni-Cu shape memory alloys. Metallurgical and Materials Transactions A, 31 (10): 2423-2430.

[7] Lee J.H., Nam T.H., Ahn H.J., Kim Y.W. 2006. Shape memory characteristics and superelasticity of Ti–45Ni–5Cu alloy ribbons. Materials Science and Engineering: A, 438-440: 691-694.

[8] Nam T.H., Saburi T., Shimizu K. 1990. Cu-Content Dependence of Shape Memory Characteristics in Ti-Ni-Cu Alloys. Materials Transactions, JIM, 31 (11): 959-967.

[9] Nam T.-H., Noh J.P., Hur S.G., Kim J.S., Kang S.B. 2002. Phase Transformation Behavior and Shape Memory Characteristics of Ti-Ni-Cu-Mo Alloys. Materials Transactions, 43 (5): 802-808.

[10] Morakabati M., Kheirandish Sh., Aboutalebi M., Karimi T.A., Abbasi S.M. 2010. The effect of Cu addition on the hot deformation behavior of NiTi shape memory alloys. Journal of Alloys and Compounds, 499 (1): 57-62.

[11] Colombo S., Cannizzo C., Gariboldi F., Airoldi G. 2006. Electrical resistance and deformation during the stress-assisted two-way memory effect in $Ni_{45}Ti_{50}Cu_5$ alloy. Journal of Alloys and Compounds, 422 (1-2): 313-320.

[12] Otsuka K., Ren X. 1999. Recent developments in the research of shape memory alloys. Intermetallics, 7 (5): 511-528.

[13] Luo Y.Y., Zhao Y.Q., Lu Y.F., Xi Z.P., Zeng W.D. 2013. Microstructure and damping characteristics of $Ti_{50}Ni_{24.9}Cu_{25}Y_{0.1}$ shape memory alloy. Materials Letters, 95: 125-127.

[14] Liu M.Y., Qi W.Y., Tong Y.X., Tian B., Chen F., Li L. 2018. Study of martensitic transformation in TiNiCuNb shape memory alloys using dynamic mechanical analysis. Vacuum, 155: 358-360.

[15] Kim W.C., Kim Y.J., Kim J.S., Na M.Y., Kim W.T., Kim D.H. 2019. Correlation between the thermal and superelastic behavior of $Ni_{50-x}Ti_{35}Zr_{15}Cu_x$ shape memory alloys. Intermetallics, 107: 24-33.

[16] Nespoli A., Villa E., Passaretti F. 2019. Effect of annealing on the microstructure of Yttrium-doped NiTiCu shape memory alloys. Journal of Alloys and Compounds, 779: 30-40.

[17] Meng X.L., Li H., Cai W., Hao S.J., Cui L.S. 2015. Thermal cycling stability mechanism of $Ti_{50.5}Ni_{33.5}Cu_{11.5}Pd_{4.5}$ shape memory alloy with near-zero hysteresis. Scripta Materialia, 103: 30-33.

[18] Sun K., Yi X., Sun B., Gao W., Wang H., Meng X., Cai W., Zhao L. 2019. The effect of Hf on the microstructure, transformation behaviors and the mechanical properties of Ti-Ni-Cu shape memory alloys. Journal of Alloys and Compounds, 772: 603-611.

[19] Miyamoto H., Taniwaki T., Ohba T., Otsuka K., Nishigori S., Kato K. 2005. Two-stage B2–B19–B19′ martensitic transformation in a $Ti_{50}Ni_{30}Cu_{20}$ alloy observed by synchrotron radiation. Scripta Materialia, 53 (2): 171-175.

[20] Fabregat-Sanjuan A., Ferrando F., De la Flor S. 2015. Influence of Heat Treatment on Internal Friction Spectrum in NiTiCu Shape Memory Alloy. Materials Today: Proceedings, 2: 755-S758.

[21] Goryczka T., Humbeeck J. 2006. Characterization of a NiTiCu shape memory alloy produced by powder technology. Journal of Achievements in Materials and Manufacturing Engineering, 17 (1-2): 65-68.

[22] Wang Z.G., Zu X.T., Huo Y. 2005. Effect of heating/cooling rate on the transformation temperatures in TiNiCu shape memory alloys. Thermochimica Acta, 436 (1-2): 153-155.

[23] Zengin R., Ozgen S., Ceylan M. 2004. Oxidation behaviour and kinetic properties of shape memory $CuAl_xNi_4$ (x=13.0 and 13.5) alloys. Thermochimica Acta, 414 (1): 79-84.

[24] Yildiz K., Balci E., Akpinar S. 2017. Quenching media effects on martensitic transformation, thermodynamic and structural properties of Cu–Al–Fe–Ti high-temperature shape memory alloy. Journal of Thermal Analysis and Calorimetry, 129 (2): 937-945.

[25] Nurveren K., Akdoğan A., Huang W.M. 2008. Evolution of transformation characteristics with heating/cooling rate in NiTi shape memory alloys. Journal of Materials Processing Technology, 196 (1-3): 129-134.

[26] Dagdelen F., Kok M., Qader I. 2019. Effects of Ta Content on Thermodynamic Properties and Transformation Temperatures of Shape Memory NiTi Alloy. Metals and Materials International, https://doi.org/10.1007/s12540-019-00298-z: 1-8.

[27] Kök M., Ahmed Zardawi H.S., Qader I.N., Kanca M.S. 2019. The effects of cobalt elements addition on Ti_2Ni phases, thermodynamics parameters, crystal structure and transformation temperature of NiTi shape memory alloys. The European Physical Journal Plus, 134 (5):197.

[28] Qader I.N., Kök M., Dağdelen F. 2019. Effect of heat treatment on thermodynamics parameters, crystal and microstructure of (Cu-Al-Ni-Hf) shape memory alloy. Physica B: Condensed Matter, 553: 1-5.

[29] Ramaiah K.V., Saikrishna C.N., Gouthama, Bhaumik S.K. 2014. $Ni_{24.7}Ti_{50.3}Pd_{25.0}$ high temperature shape memory alloy with narrow thermal hysteresis and high thermal stability. Materials & Design (1980-2015), 56: 78-83.

[30] Kök M., Yakinci Z.D., Aydoğdu A., Aydoğdu Y. 2014. Thermal and magnetic properties of Ni51Mn28.5Ga19.5B magnetic-shape-memory alloy. Journal of Thermal Analysis and Calorimetry, 115 (1): 555-559.

[31] Dagdelen F., Ercan E. 2014. The surface oxidation behavior of Ni–45.16%Ti shape memory alloys at different temperatures. Journal of Thermal Analysis and Calorimetry, 115 (1): 561-565.

[32] Acar E. 2016. TiNi akıllı alaşımlarında faz dönüşüm özellikleri. Gazi Üniversitesi Fen Bilimleri Dergisi Part C: Tasarım ve Teknoloji, 4 (3): 165-171.

[33] de Araújo C.J., da Silva N.J., Da Silva M.M., Gonzalez C.H. 2011. A comparative study of Ni–Ti and Ni–Ti–Cu shape memory alloy processed by plasma melting and injection molding. Materials & Design, 32 (10): 4925-4930.

[34] Thomasová M., Seiner H., Sedlak P., Frost M., Sevcik M., Szurman I., Kocich R., Drahokoupil J., Sittner P., Landa M. 2017. Evolution of macroscopic elastic moduli of martensitic polycrystalline NiTi and NiTiCu shape memory alloys with pseudoplastic straining. Acta Materialia, 123: 146-156.